Laser Physics, Vol. 14, No. 4, 2004, pp. 615–620.

(De)coherence Physics with Condensates in Microtraps

C. Henkel[1], S. A. Gardiner[2], and A. Negretti[1, 3]

[1] *Institut für Physik, Universität Potsdam, Potsdam, 14469 Germany*
e-mail: carsten.henkel@quantum.physik.uni-potsdam.de

[2] *Clarendon Laboratory, Department of Physics, University of Oxford, Oxford, OXI 3PU United Kingdom*

[3] *Dipartimento di Fisica, Università di Trento, Povo (TN), 38050 Italy, and ECT*, Villazzano (TN), 38050 Italy*

Received September 25, 2003

Abstract—We discuss the dynamics of a condensate in a miniaturized electromagnetic trap formed above a microstructured substrate. Recent experiments have found that trap lifetimes get reduced when approaching the substrate because atoms couple to thermally excited near fields. The data agree quantitatively with our theory [Appl. Phys. B **69**, 379 (1999)]. We focus on the decoherence of a quantum degenerate gas in a quasi-one-dimensional trap. Monte Carlo simulations indicate that atom interactions reduce the condensate decoherence rate. This is explained by a simple theory in terms of the suppression of long-wavelength excitations. We present preliminary simulation results for the adiabatic generation of dark solitons.

1. INTRODUCTION

Atom chips hold great promise for the implementation of a scalable neutral atom quantum computer and are currently realized in a number of laboratories [1, 2]. In recent experiments, electromagnetic traps are formed from microstructured wire patterns deposited on a solid surface. The concept is well adapted to miniaturization as lower currents lead to steeper magnetic potentials; trap arrays operating in parallel are also implemented in a straightforward way. A key issue for applications in atom interferometry [3, 4] and quantum information processing is decoherence, since the trapped atoms couple to a macroscopic, "hot" substrate nearby. The coupling is mediated by magnetic near field fluctuations that are generated by thermal charge and polarization fluctuations in the substrate and leak out of it. This magnetic noise has a broad band spectrum, and the induced spin flips drive trap loss, as predicted by one of the present authors in [5]. It has recently been observed in the group of E.A. Hinds [6], and quantitative agreement with the theory has been found by the group of E.A. Cornell [7].

In this contribution, we discuss a simple decoherence scenario for Bose–Einstein-condensed atomic matter waves. We neglect trap loss and focus on the in-trap perturbation due to magnetic field fluctuations. After a review of near field noise above a thermal substrate, Monte Carlo simulations for the condensate order parameter in a fluctuating field are described. The data are compared to a kinetic two-component theory and show that, already for moderate interaction parameters, condensates are more robust with respect to fluctuations.

2. MODEL

We consider an elongated trap similar to those formed above current carrying wires [1, 2] and describe the matter waves in a one-dimensional mean field approximation [8] (units with $\hbar = m = 1$),

$$i\partial_t\psi = -\frac{1}{2}\partial_x^2\psi + V(x,t)\psi + g|\psi(x,t)|^2\psi, \qquad (1)$$

where the interaction parameter $g = 2\Omega_r a$ depends on the transverse confinement frequency Ω_r and the three-dimensional scattering length a [9]. The density $|\psi(x,t)|^2$ is normalized to the total number of particles N. The potential $V(x,t)$ determines the dynamics in the axial direction. We assume that, for $t < 0$, the atoms are confined in a harmonic trap with frequency Ω and occupy all the zero-temperature condensate modes $\phi_0(x)$. For $t \geq 0$, the axial confinement is switched off, the atoms expand, and we take into account their interaction with magnetic field fluctuations by letting $V(x,t)$ be a random potential. Note that the transverse potential is kept constant. Equation (1) thus describes the interplay between matter wave interactions and time-dependent noise in an essentially one-dimensional geometry. In contrast to previous work in the field of nonlinear random waves [10, 11], our initial condition does not correspond to a self-contained soliton because we assume repulsive interactions $g > 0$. Current experiments in wire traps have been hampered by the presence of a static field modulation that leads to fragmentation of the expanding atom cloud [12, 13]. This makes a direct comparison to our model problematic.

2.1. Magnetic Noise

If for simplicity we ignore spin flip processes, thermal magnetic noise translates into a random potential determined by the field component parallel to the (static) magnetic field at the trap center and the magnetic moment,

$$V(x,t) = \mu\delta B_\parallel(x,t). \qquad (2)$$

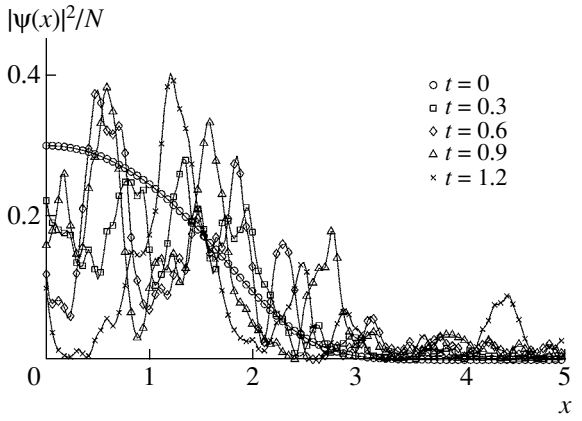

Fig. 1. Expansion of a self-interacting Schrödinger field in a noisy potential, single realization. The normalized spatial density is plotted at different times given in the inset. Parameters in Eq. (1): interaction strength $gN = 10$, noise strength $\gamma = 1$, and correlation length $l_{\mathrm{corr}} = 0.1$. Harmonic oscillator units with respect to the initial confinement frequency Ω are used: $t \mapsto \Omega t$, $x \mapsto (\hbar/m\Omega)^{1/2}x$. The numerical solution uses a discrete space-time grid with time step $\Omega dt = 0.1$ and 2^{14} space points spaced $dx = 0.0294$ units. The time evolution is computed with a split-operator algorithm.

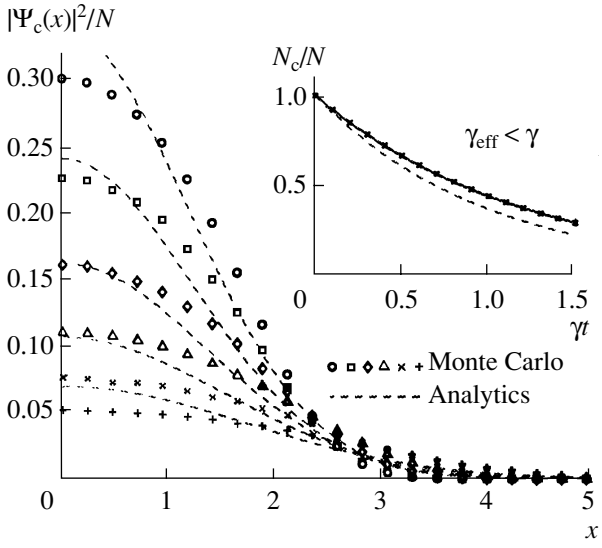

Fig. 2. Normalized density profiles of the coherent (noise-averaged) field. From top to bottom, the profiles are taken at $t = 0, 0.3, \ldots 1.5$. Inset: coherent fraction (relative particle number). Symbols: Monte Carlo results, dashed lines; Gaussian approximation (8), solid line; exponential decay with renormalized decoherence rate $\gamma_{\mathrm{eff}} = 0.82\gamma$. Same units and parameters as in Fig. 1.

For a microtrap above a planar substrate with temperature T_s and resistivity ϱ, the theory developed in [5, 14] gives the following approximate correlation function:

$$\langle V(x,t)V(x',t')\rangle \approx \gamma\delta(t-t')C(|x-x'|), \qquad (3)$$

$$\gamma = \frac{\mu^2\mu_0^2 k_B T_s}{16\pi\hbar^2\varrho z_t}, \qquad (4)$$

$$C(|x-x'|) = \frac{l_{\mathrm{corr}}^2}{l_{\mathrm{corr}}^2 + (x-x')^2}, \qquad (5)$$

where the notation is that of [5]; the rate γ would correspond to the phase diffusion rate if the potential fluctuated only in time (γ is written in SI units for convenience), and z_t is the height of the trap above the substrate. The spatial correlation length l_{corr} is comparable to z_t [14]; a typical value is a few microns. For a discussion of the height dependence $\propto 1/z_t$ and corrections involving the substrate skin depth, see [5]. These corrections are required to describe quantitatively the spin flip losses observed in microtraps [7]. Note in this context that the correlation function (3) is computed by keeping only a frequency range up to typical transition frequencies in the microtrap. In our one-dimensional framework, these are necessarily smaller than the radial oscillation frequency Ω_r. On the corresponding time scales, magnetic noise is approximately white [15].

2.2. Coherence Functions

Our model (1) is a "classical" nonlinear field equation in a stochastic potential. We shall therefore compute averages with respect to realizations of the noise potential [10], as explained below. We also comment on the relation of our approach to the quantum field theory behind Bose–Einstein condensation [8, 16].

For a single, typical realization of the noise, the density $n(x, t) = |\psi(x, t)|^2$ and its temporal evolution is shown in Fig. 1. A complicated fringe pattern appears due to the interference between the expanding condensate mode and the excitations generated by noise. The fringe phase depends on the history of the noise, so that, after averaging, a smooth average field $\psi_c(x, t) \equiv \langle\psi(x, t)\rangle$ with a decaying weight emerges (Fig. 2). This quantity would be revealed in a homodyne measurement of the condensate by mixing it with a reference atom beam without fluctuations and by repeating the experiment over many realizations of the noise. We shall call it the "coherent field" in the following. Its absolute phase is fixed by the phase of the initial wave function $\phi_0(x)$. Note that the coherent field is quite analogous to the condensate order parameter in the symmetry breaking approach to Bose condensation when $N_c \sim N$ [16]. Since the equation of motion for the atomic quantum field is essentially given by Eq. (1), with classical fields replaced by operators, classical simulations are also able to capture some aspects of quantum (and thermal) field fluctuations; for example, in the initial state, one may include randomly chosen amplitudes for the lowest excitation modes of the trapped condensate (see, e.g., [17, 18, 19, 20]).

Another condensate definition, which is also applicable in $U(1)$ covariant theories, is based on long-range order in the single-particle density matrix [21]. This quantity corresponds in our problem to the coherence function $\rho(x, x', t) \equiv \langle \psi^*(x, t)\psi(x', t)\rangle$. It gives the fringe contrast in a double-slit experiment with slit positions x and x' in the matter wave field [22, 23]. In the context of decoherence theory, a central concept is the spatial coherence length $l_{\rm coh}(t)$, i.e., the width of the coherence function $\rho(x, x', t)$ with respect to $s = x - x'$ [24, 25]: two points in the matter wave no longer interfere when their separation becomes larger than $l_{\rm coh}(t)$. Alternatively, one can show that the momentum distribution, averaged over many realizations, is proportional to the Fourier transform of the spatially averaged coherence function $\Gamma(s, t)$ with respect to s, where

$$\Gamma(s, t) = \int dx \rho(x, x + s, t). \quad (6)$$

This gives the well-known relation $l_{\rm coh}\delta p \sim \hbar$, where δp is the width in momentum. The reduction of the coherence length ("decoherence") is borne out in the results plotted in Fig. 3. Long-range coherence is also visible in this figure: a fraction of the bosonic wave field is coherent across the full cloud size. We show elsewhere that this fraction can be identified with the coherent field $\langle \psi(x, t)\rangle$, reinforcing the analogy between the condensate order parameter and the noise-averaged nonlinear Schrödinger field.

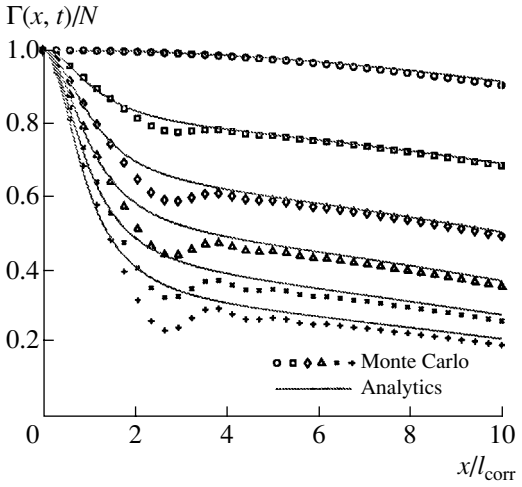

Fig. 3. Spatially averaged coherence function [Eq. (6)] for different expansion times (t = 0, 0.3, …1.5, as in Fig. 2). Symbols: Monte Carlo results, solid lines: kinetic theory with renormalized decoherence rate $\gamma_{\rm eff} = 0.82\gamma$ and noise correlation length $l_{\rm eff} = 1.25 l_{\rm corr}$. Other parameters same as in Fig. 1. The oscillations are attributed to the Thomas–Fermi density kink at the border of the coherent field that is not captured by the Gaussian ansatz (8) used in the kinetic theory.

3. KINETIC THEORY

3.1. Basic Equations

In the two-component model of Bose–Einstein condensation, the condensate evolves according to a nonlinear Schrödinger equation including loss terms and interactions with the noncondensed density. The noncondensed component is described by a suitable kinetic theory that often neglects interactions [8, 26–28]. We have adapted this model to our problem of an expanding condensate by replacing the average with respect to the density operator of the field by the average over the evolutions in an ensemble of random potentials. For a similar approach, see [29]; the noninteracting case has been treated in [30]. An essentially analytical solution has been obtained with two approximations: (i) we describe the noncondensed atoms (the fluctuations around the coherent field) by the free space dispersion relation, and (ii) we neglect in the nonlinear Schrödinger equation the interaction between the condensate (more precisely, the coherent field) and its fluctuations. We focus here on the dynamics of the coherent field; condensate fluctuations will be discussed elsewhere. The resulting equation is

$$i\partial_t \psi_{\rm c} = -\frac{1}{2}\partial_x^2 \psi_{\rm c} + g|\psi_{\rm c}(x, t)|^2 \psi_{\rm c} - \frac{i\gamma}{2}\psi_{\rm c}, \quad (7)$$

where the loss rate γ is given by the noise spectrum (3) according to the Furutsu–Novikov theorem [10]. This equation can be solved approximately with a time-dependent Thomas–Fermi profile [31, 32] or a Gaussian ansatz [33, 34]. We follow the latter method because it simplifies the calculation of coherence functions and get the coherent density

$$|\psi_{\rm c}(x, t)|^2 = \frac{N}{\sqrt{2\pi}u(t)} e^{-\gamma t} \exp[-x^2/(2u^2(t))], \quad (8)$$

where N is the total number of atoms and $u(t)$, the condensate spatial width, is the solution of

$$\ddot{u} = -\frac{\partial}{\partial u}\left(\frac{1}{8u^2} + \frac{\tilde{g}(t)}{u}\right). \quad (9)$$

The effective interaction strength is $\tilde{g}(t) = gNe^{-\gamma t}/(4\sqrt{\pi})$, and the initial condition $u(0)$ minimizes $U_{\rm eff}(u) = 1/(8u^2) + \tilde{g}(0)/u + \frac{1}{2}\Omega^2 u^2$, where Ω is the frequency of the initial axial trapping potential. [In SI units, $U_{\rm eff}(u) = \hbar^2/(8mu^2) + \tilde{g}(0)/u + \frac{1}{2}m\Omega^2 u^2$, and similar changes apply to Eq. (9).]

3.2. Comparison to Numerical Simulations

The simple kinetic theory outlined above captures qualitatively the features observed in Monte Carlo simulations of Eq. (1), as shown by Figs. 2 and 3. We attribute deviations to the approximate treatment of interactions in the theory.

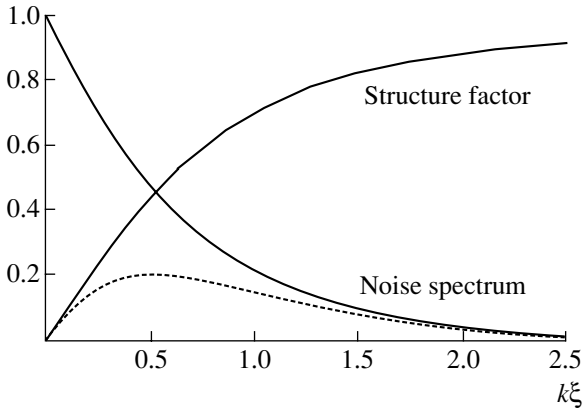

Fig. 4. Static structure factor $S(k; n_c)$ (homogeneous condensate with density n_c), noise spectral density $S_V(k)$, and effective excitation rate $S(k; n_c)S_V(k)$ (dashed solid line) vs. quasiparticle wave vector k. The noise spectrum is the Fourier transform of the correlation function (5) with a correlation length $l_{corr} = 1.5\xi$; it is normalized to $S_V(k = 0) = 1$. Wave vectors are normalized to the inverse healing length $1/\xi = \sqrt{4gn_c}$.

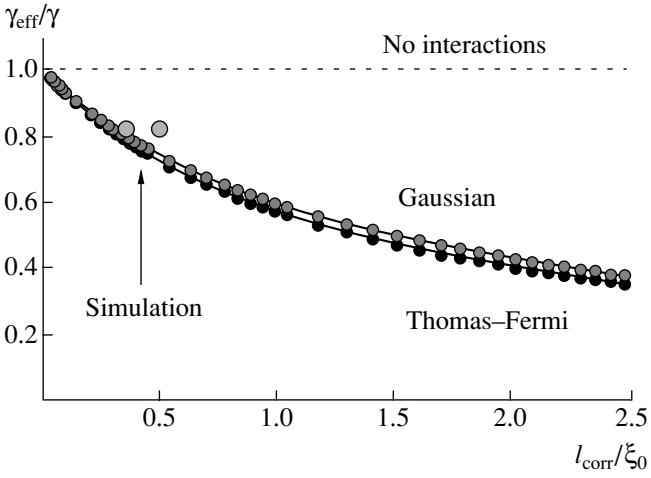

Fig. 5. Renormalized decoherence rate γ_{eff} for increasing interaction strength. On the x-axis is plotted the ratio $l_{corr}/\xi_0 \propto \sqrt{g}$, where ξ_0 is the healing length at the condensate center, $\xi_0 = 1/\sqrt{4gn_c(x = 0)}$. Large dots: Monte Carlo data (see text). Dark (grey) dots: prediction of local density approximation integrated over a Thomas–Fermi (gaussian) density profile. The decoherence rate is normalized to its value γ in an ideal gas.

The density profile of the coherent field is not exactly Gaussian because, for the chosen parameters, one already approaches the Thomas–Fermi regime. The coherent fraction of particles $N_c(t)/N = (1/N)\int dx\,|\psi_c(x, t)|^2$, however, shows an exponential decay, as predicted by Eq. (7). We find quantitative agreement with the kinetic theory when a "renormalized" decay rate $\gamma_{eff} < \gamma$ is used. Further simulation runs show that the ratio γ_{eff}/γ does not change significantly when the noise strength is reduced by an order of magnitude. An analytical approximation for γ_{eff}/γ is derived below.

3.3. Renormalized Decoherence Rate

It is intuitively clear that the decoherence rate is related to the number of excitations created per unit time by the fluctuating potential. In a homogeneous condensate driven by a spatially periodic potential, this excitation rate is proportional to the structure factor $S[k; n_c]$, where k is the wave vector of the excitation and n_c is the condensate density [16]. Bogoliubov theory gives the well-known expression

$$S[k; n_c] = \frac{|k|}{\sqrt{k^2 + 4gn_c}}. \qquad (10)$$

For wave vectors smaller than the inverse healing length $1/\xi = (4gn_c)^{1/2}$, condensate excitations are suppressed, which is typical behavior for a superfluid. In the opposite limit $|k|\xi \gg 1$, $S[k; n_c] \longrightarrow 1$ and the excitations behave like free particles (see Fig. 4).

We describe in our problem the reduced depletion of the coherent field by including the structure factor in the scattering cross section due to the noise potential using a local density approximation. The magnitude of the reduction is determined by the competition between the wave vector scales $1/l_{corr}$ (width of the noise spectrum) and $1/\xi(x)$ (local healing length): at small k, the structure factor renders the excitation of the matter wave field less efficient. Details will be reported elsewhere; results for the normalized depletion rate γ_{eff}/γ are plotted in Fig. 5. The strength of the interactions is expressed in terms of the ratio l_{corr}/ξ_0, where the healing length ξ_0 is taken at the condensate center. Both Thomas–Fermi and Gaussian density profiles give very similar results. The ideal gas value $\gamma_{eff} = \gamma$ is recovered for $\xi_0 = \infty$, but since $\xi_0 \propto g^{-1/2}$, the next order corrections already come into play for moderate interaction parameters g. Very strong interactions, where $\xi_0 \longrightarrow 0$, significantly slow down decoherence. The decoherence rate extracted from the Monte Carlo results is fairly well reproduced by this approach. The two data points we have plotted correspond to two values for the healing length: based either on the numerically computed condensate density or on its Thomas–Fermi approximation.

Let us finally note that, for large interactions or long expansion times, the coupling of the coherent field to the noncondensed fraction will no longer be negligible compared to the random potential and our approximate solution will lose accuracy. In this limit, we may expect that noise-induced decoherence is replaced by an "open

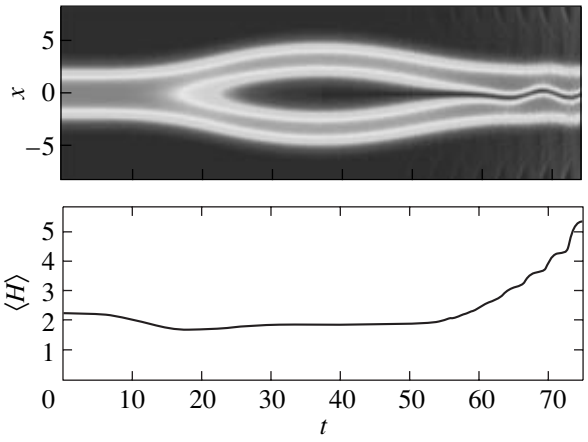

Fig. 6. Top: splitting and recombining a condensate in a time-dependent potential. At full separation, a 0.98π phase difference is imprinted on the interferometer arms. The condensate starts in the trap ground state and merges into a dark soliton that oscillates in the trap and radiates sound waves. Bottom: average value of the energy per particle vs. time. Harmonic oscillator units with respect to the initial harmonic potential (frequency Ω) are used. At maximum separation, the double wells are 4 units apart, with a barrier of height $8\hbar\Omega$ in between; the oscillation frequencies at both well bottoms are then $\sqrt{2}\Omega$. Numerical parameters: $gN = 5$, 4×10^4 time steps with $\Omega dt = 0.00175$, and 2^7 space points spaced $dx = 0.3$ units.

system dynamics" similar to the models discussed for a condensate at finite temperature [35, 36, 37].

4. CONCLUSIONS AND OUTLOOK

We have shown that weak magnetic field fluctuations are present in the near field of metallic substrates and perturb the coherent evolution in atom chips. Recent experiments have quantitatively confirmed the predictions of this scenario. A quantum kinetic theory for a degenerate trapped boson gas subject to noise has been worked out in the mean field approximation and solved analytically. The comparison to numerical simulations demonstrates that interatomic interactions reduce the coherence rate relative to the noncondensed case. We have suggested an explanation in terms of the structure factor of a quasi-homogeneous system that leads to an accurate agreement with the numerical data.

Further investigations will address the renormalization of the noise correlation length due to interactions and the impact of finite temperature in the initial condensate. Another route of research will follow the decoherence of trapped condensate interferometers [3, 4] subject to noise. Preliminary numerical results for the splitting and recombining of a condensate in a slowly deformed trap are shown in Fig. 6. At the middle of the process, a 0.98π phase difference is imprinted on the separated arms. The recombination then leads to an antisymmetric, dark soliton state that starts to oscillate in the trap [38–40]. Note that the condensate splitting allows us to perform the phase imprint with minimum perturbations because the field amplitude is zero where the phase jumps. Hence the condensate mean energy does not change immediately, but only when the arms are adiabatically recombined. This system offers a delicate control over the soliton preparation and may be useful to study the interactions between solitons and sound waves that have attracted interest recently [41, 42].

ACKNOWLEDGMENTS

S.A.G. thanks the Alexander von Humboldt foundation for a fellowship. A.N. acknowledges support from the European Union network FAST-Net (contract no. HPRN-CT-2002-00304). C. H. is indebted to Martin Wilkens for continuous support.

REFERENCES

1. R. Folman, P. Krüger, J. Schmiedmayer, *et al.*, Adv. At. Mol. Opt. Phys. **48**, 263 (2002).
2. J. Reichel, Appl. Phys. B **74**, 469 (2002).
3. E. A. Hinds, C. I. Vale, and M. G. Boshier, Phys. Rev. Lett. **86**, 1462 (2001).
4. E. Andersson, T. Calarco, and R. Folman, *et al.*, Phys. Rev. Lett. **88**, 100401 (2002).
5. C. Henkel, S. Pötting, and M. Wilkens, Appl. Phys. B **69**, 379 (1999).
6. M. P. A. Jones, C. J. Vale, D. Sahagun, *et al.*, Phys. Rev. Lett. **91**, 080401 (2003).
7. D. M. Harber, J. M. McGuirk, J. M. Obrecht, and E. A. Cornell, J. Low Temp. Phys. **133**, 229 (2003); D. M. Harber, personal communication (2003).
8. A. L. Fetter, in *Bose–Einstein Condensation in Atomic Gases*, Ed. by M. Inguscio, S. Stringari, and C. E. Wieman (IOS Press, Amsterdam, 1999).
9. M. Olshanii, Phys. Rev. Lett. **81**, 938 (1998).
10. V. V. Konotop and L. Vázquez, *Nonlinear Random Waves* (World Sci., Singapore, 1994).
11. *Nonlinearity and Disorder: Theory and Applications*, Ed. by F. Abdullaev, O. Bang, and M. P. Sørensen (Kluwer Academic, Dordrecht, 2001), NATO Sci. Ser. II, Math. Phys. Chem., Vol. 45.
12. S. Kraft, A. Günther, H. Ott, *et al.*, J. Phys. B **35**, L469 (2002).
13. A. E. Leanhardt, Y. Shin, A. P. Chikkatur, *et al.*, Phys. Rev. Lett. **90**, 100404 (2003).
14. C. Henkel, K. Joulain, R. Carminati, and J.-J. Greffet, Opt. Commun. **186**, 57 (2000).
15. C. Henkel, P. Krüger, R. Folman, and J. Schmiedmayer, Appl. Phys. B **76**, 173 (2003).
16. F. Dalfovo, S. Giorgini, L. P. Pitaevskii, and S. Stringari, Rev. Mod. Phys. **71**, 463 (1999).
17. Y. Castin and R. Dum, Phys. Rev. A **57**, 3008 (1998).
18. S. Dettmer, D. Hellweg, P. Ryytty, *et al.*, Phys. Rev. Lett. **87**, 160406 (2001).

19. M. J. Davis, R. J. Ballagh, and K. Burnett, J. Phys. B **34**, 4487 (2001).
20. K. Goral, M. Gajda, and K. Rzazewski, Phys. Rev. A **66**, 051602(R) (2002).
21. A. J. Leggett, Rev. Mod. Phys. **73**, 307 (2001).
22. L. Mandel and E. Wolf, *Optical Coherence and Quantum Optics* (Cambridge Univ. Press, Cambridge, 1995).
23. S. Richard, F. Gerbier, J. H. Thywissen, *et al.*, Phys. Rev. Lett. **91**, 010405 (2003).
24. W. H. Zurek, Phys. Today **44** (10), 36 (1991).
25. D. Giulini, E. Joos, C. Kiefer, *et al.*, *Decoherence and the Appearance of a Classical World in Quantum Theory* (Springer, Berlin, 1996).
26. C. W. Gardiner, P. Zoller, R. J. Ballagh, and M. J. Davis, Phys. Rev. Lett. **79**, 1793 (1997).
27. D. Jaksch, C. W. Gardiner, K. M. Gheri, and P. Zoller, Phys. Rev. A **58**, 1450 (1998).
28. H. T. C. Stoof, J. Low Temp. Phys. **114**, 11 (1999).
29. A. B. Kuklov and J. L. Birman, Phys. Rev. A **63**, 013609 (2000).
30. A. M. Jayannavar and N. Kumar, Phys. Rev. Lett. **48**, 553 (1982).
31. Y. Castin and R. Dum, Phys. Rev. Lett. **77**, 5315 (1996).
32. P. Öhberg and L. Santos, Phys. Rev. Lett. **89**, 240402 (2002).
33. V. Pérez-García, H. Michinel, J. I. Cirac, *et al.*, Phys. Rev. A **56**, 1424 (1997).
34. H. T. C. Stoof, J. Stat. Phys. **87**, 1353 (1997).
35. J. Anglin, Phys. Rev. Lett. **79**, 6 (1997).
36. R. Graham, Phys. Rev. Lett. **81**, 5262 (1998).
37. R. A. Duine and H. T. C. Stoof, Phys. Rev. A **65**, 013603 (2002).
38. R. Dum, J. I. Cirac, M. Lewenstein, and P. Zoller, Phys. Rev. Lett. **80**, 2972 (1998).
39. T. Busch and J. R. Anglin, Phys. Rev. Lett. **84**, 2298 (2000).
40. S. Burger, K. Bongs, S. Dettmer, *et al.*, Phys. Rev. Lett. **83**, 5198 (1999).
41. N. G. Parker, N. P. Proukakis, M. Leadbeater, and C. S. Adams, Phys. Rev. Lett. **90**, 220401 (2003).
42. J. Dziarmaga, Z. P. Karkuszewski, and K. Sacha, J. Phys. B **36**, 1217 (2003).